

Journal of Visualized Experiments

Direct Stochastic Optical Reconstruction Microscopy of Extracellular Vesicles in Three Dimensions

--Manuscript Draft--

Article Type:	Invited Methods Collection - JoVE Produced Video
Manuscript Number:	JoVE62845R2
Full Title:	Direct Stochastic Optical Reconstruction Microscopy of Extracellular Vesicles in Three Dimensions
Corresponding Author:	Dirk Dittmer, Ph.D. University of North Carolina at Chapel Hill School of Medicine Chapel Hill, NC UNITED STATES
Corresponding Author's Institution:	University of North Carolina at Chapel Hill School of Medicine
Corresponding Author E-Mail:	dirk_dittmer@med.unc.edu
Order of Authors:	Meredith Chambers Ryan McNamara Dirk Dittmer, Ph.D.
Additional Information:	
Question	Response
Please specify the section of the submitted manuscript.	Biology
Please indicate whether this article will be Standard Access or Open Access.	Standard Access (\$1400)
Please indicate the city, state/province, and country where this article will be filmed . Please do not use abbreviations.	Chapel Hill, North Carolina, United States of America
Please confirm that you have read and agree to the terms and conditions of the author license agreement that applies below:	I agree to the Author License Agreement
Please provide any comments to the journal here.	
Please confirm that you have read and agree to the terms and conditions of the video release that applies below:	I agree to the Video Release

TITLE:

Direct Stochastic Optical Reconstruction Microscopy of Extracellular Vesicles in Three Dimensions

AUTHORS AND AFFILIATIONS:

Meredith G. Chambers, Ryan P. McNamara, Dirk P. Dittmer

¹Department of Microbiology and Immunology, Lineberger Comprehensive Cancer Center, The University of North Carolina at Chapel Hill School of Medicine, Chapel Hill, 27599

Corresponding Author:

Dirk P. Dittmer (dirk_dittmer@med.unc.edu)

Email Addresses of Co-Authors:

Meredith G. Chambers (merecham@live.unc.edu)

Ryan P. McNamara (ryanpm@email.unc.edu)

Dirk P. Dittmer (dirk_dittmer@med.unc.edu)

SUMMARY:

Direct stochastic optical reconstruction microscopy (dSTORM) is used to bypass the typical diffraction limit of light microscopy and to view exosomes at the nanometer scale. It can be employed in both two and three dimensions to characterize exosomes.

ABSTRACT:

Extracellular vesicles (EVs) are released by all cell types and play an important role in cell signaling and homeostasis. The visualization of EVs often require indirect methods due to their small diameter (40–250 nm), which is beneath the diffraction limit of typical light microscopy. We have developed a super-resolution microscopy-based visualization of EVs to bypass the diffraction limit in both two and three dimensions. Using this approach, we can resolve the three-dimensional shape of EVs to within +/- 20 nm resolution on the XY-axis and +/- 50 nm resolution along the Z-axis. In conclusion, we propose that super-resolution microscopy be considered as a characterization method of EVs, including exosomes, as well as enveloped viruses.

INTRODUCTION:

Extracellular vesicles (EVs) are membrane-bound vesicles released by all cell types. They contain lipids, proteins, metabolites, and nucleic acids and transfer these materials locally between cells and distally between tissues and organs. There are three primary subtypes of EVs: apoptotic bodies, microvesicles, and exosomes^{1,2}. Here, we focus our discussion on exosomes and their associated proteins.

Exosomes are secreted vesicles originating from the inward budding of early endosomes into the multivesicular body (MVB). The MVB then fuses with the plasma membrane, releasing the exosomes into the extracellular space to travel to other cells^{3,4}. Exosomes exist on a spectrum of sizes ranging from 40 to 150 nm and are enriched with endosomal transmembrane proteins known as tetraspanins (CD9, CD63, CD81), membrane-bound endosomal sorting complex

required for the transport (ESCRT), and lipid raft-associated proteins^{1,2, 5–7}.

Characterizing the biochemical makeup of exosomes has become a popular field for researchers to better understand their functional nature. Many methods exist for visualizing and characterizing exosomes, including nanoscale flow cytometry, nanoparticle tracking analysis (NTA), scanning and transmission electron microscopy (TEM), surface plasmon resonance, resistive pulse sensing, and traditional light microscopy, each of which contains intrinsic pros and cons^{8,9}. TEM and cryo-EM can achieve nanometer-based resolution, but often require dehydrating and freeze-fracture steps, thereby shrinking or lysing EVs^{10,11}. NTA relies on light scattering, allowing for the characterization of hundreds of EVs at a time, but is an indirect measurement of particle size and cannot easily distinguish between EVs, viruses, and protein aggregates^{12–16}. Nanoscale flow cytometry employs light scattering from an excitation path, which can then be translated into size measurements, but is an emerging technology, and there is little consensus on what size of particles are within the linear range of detection for various instruments^{12,17,18}.

Traditional light microscopy using fluorescent proteins or dyes has been one of the most heavily employed techniques for visualizing subcellular compartments, protein complexes, and signaling machinery within a cell. While this technique proves useful in visualizing the localization of complexes, the diffraction limit of traditional light microscopy (around 250–400 nm) prevents the clear resolution of proteins or structures in the typical size range of an exosome (40–150 nm)^{12,19,20}.

Super-resolution microscopy, namely, direct stochastic optical reconstruction microscopy (dSTORM), distinguishes itself from conventional light microscopy by employing the photoswitchable properties of specific fluorophores and detecting these blinking events to reconstruct images down to nanometer precision²¹. Photoswitching events are collected using a high-framerate detection camera over the course of tens of thousands of individual exposures, and a point spread function is used to map with high confidence the exact location of the photoswitching fluorophore^{19,20,22}. This allows dSTORM to bypass the diffraction limit of light microscopy. Several groups have reported the use of super-resolution techniques for visualizing and tracking exosomes and their associated proteins^{22–25}. The final resolution depends on the biophysical properties of the fluorophore, but often ranges from +/-10–100 nm along the XY-axis, allowing single-molecule resolution.

The ability to resolve individual fluorophores at this scale on the XY-axis has revolutionized microscopy. However, there is little data on the three-dimensional (3-D) dSTORM of an exosome. Therefore, we sought to establish a standard operating procedure (SOP) for dSTORM-based visualization and characterization of purified EVs, including exosomes to nanometer precision in 3-D.

PROTOCOL:

1 Propagation and maintenance of cell lines

1.1 Acquire human osteosarcoma cells (U2OS) and place the cells in the growth medium supplemented with 10% exosome-free Fetal Bovine Serum and 1x Penicillin/Streptomycin solution.

NOTE: Exosome-free Fetal Bovine Serum was generated following the protocol presented in McNamara et. al.²⁶.

1.2 Maintain the U2OS cells in a copper-coated incubator at 37 °C in 5% CO₂ and passage cells in T175 flasks^{26,27}. The cells must be maintained in mid-logarithmic growth phase to prevent subpopulations from arising, or from the accumulation of apoptotic debris during the stationary phase.

2 Exosome isolation and purification

2.1 Grow the U2OS cell lines to full confluency in 10 separate T175 flasks with 50 mL of media per flask. Remove the cell supernatant and successively passage it through a 0.45 µm and 0.22 µm vacuum filtration apparatus.

2.2 Subject the supernatant to crossflow filtration (also known as tangential flow filtration) on a filtration system equipped with the 750 kDa hollow-fiber cartridge in order to remove smaller proteins or metabolites²⁸.

2.2.1 Passage the supernatant through the tangential flow filtration operator at a constant forward pressure of 30 psi, while maintaining a retention pressure of <20 psi to produce a Δ pressure of 10 or more psi. Place a magnetic stir bar in the retentate tank and set to 150 rpm²⁶.

2.2.2 Maintain the feed rate at 40 mL/min or higher. Collect the permeate in a reservoir and dispose of it.

2.3 Concentrate the supernatant to 30 mL, and then equilibrate with four volumes of 1x PBS. Collect the crossflow filtered and equilibrated solution in a 50 mL conical tube.

2.4 Precipitate the EVs at 4 °C overnight in a final concentration of 40 mg/mL polyethylene glycol with a molecular weight of 8,000 Da. Centrifuge the EVs at 1,200 x g at 4 °C for 1 h and resuspend in 500 µL of 1x PBS.

2.5 Incubate the EVs with 50 µg/mL of photoswitchable red membrane intercalating dye and 50 µg/mL of RNase A in 1x PBS at 4 °C for 1 h.

2.6 Remove excess dye through a column on a protein purification system attached to a fraction collector. Identify EV fractions through UV absorbance and pool them into a microcentrifuge tube²⁶.

2.7 Affinity-select a total of 200 μ L of EVs using anti-CD81 magnetic beads equilibrated in 1x PBS.

2.7.1 Dilute 100 μ L of the anti-CD81 magnetic beads in 1x PBS to a total volume of 1 mL and allow them to bind at 4 $^{\circ}$ C for 2 h in a 2 mL microcentrifuge tube with continuous rocking.

2.8 Wash the anti-CD81 beads and EV three times with 1x PBS. Elute CD81+ EV from the solution with 100 mM Glycine at pH 2.0 for 30 min at 37 $^{\circ}$ C.

2.9 Pipette the purified CD81+ EV into an equal volume of 100 mM Tris-HCl at pH 7.5 in 1x PBS.

NOTE: An aliquot of purified CD81+ EV solution may be reserved for Nanoparticle Tracking Analysis or electron microscopy in order to confirm the purity of the solution and presence of EVs²⁶.

3 Fixation and preparation

3.1 Place affinity-purified EVs onto glass-bottom μ -slide 8-well plates in a total volume of 200 μ L (can dilute EV sample in 100 mM Tris-HCl at pH 7.5 in 1x PBS) and allow to adhere to the surface overnight at 4 $^{\circ}$ C.

3.2 Without removing the existing solution from the 8-well plate, fix EVs onto the plates by adding 200 μ L of 4% paraformaldehyde in 1x PBS to the EV-containing solution in each well and allow to incubate for 30 min at room temperature²¹.

3.3 Carefully remove paraformaldehyde and excess solution with a micropipette in order to not disturb the EVs. Wash the EV with 1x PBS to remove excess paraformaldehyde. Perform the wash procedure three times. Remove excess 1x PBS.

3.4 Prepare 250 μ L of dSTORM B-cubed buffer solution per sample by creating a solution of 5 mM protocatechuate dioxygenase (Part A) diluted in imaging buffer (Part B) per manufacturer's protocol.

NOTE: The concentration of the enzyme in the buffer may be doubled to 10 mM if photobleaching occurs.

3.4.1 Add 250 μ L of the prepared buffer to each well per manufacturer's protocol for 20 min at room temperature before imaging to scavenge oxidizing molecules.

NOTE: The EV can then be either viewed immediately or stored at 4 $^{\circ}$ C for up to a week. Replace the buffer following storage before every visualization.

4 Direct stochastic optical reconstruction microscopy calibration

4.1 Prepare the beads required for the calibration of the super-resolution microscope by diluting 100 nm microspheres to a concentration of 0.5% in molecular biology grade water and pipetting 200 μ L into each well of a glass-bottom μ -slide 8-well plate.

4.1.1 Allow the beads to settle in the wells for 1 h at room temperature.

4.2 Without removing the existing solution, add 200 μ L of 4% paraformaldehyde in PBS to each well to the calibration bead solution and allow to incubate for 30 min at room temperature.

4.3 Carefully remove the paraformaldehyde with a micropipette to not disturb the beads and wash the beads three times with 1x PBS. Prepare the buffer according to step 3.4.

4.4 Remove 1x PBS and add 250 μ L of the prepared buffer to each well. Allow the buffer to sit for 20 min before visualization.

4.5 Before placing anything on the stage, connect to the 3-D microscope using the **Connect the Microscope** button. Add 100x oil to the objective and place the center of the well on top of the objective. In the **Acquire** setting, turn on the 473 and 640 nm excitation lasers and click on **View**.

4.5.1 Without the 3-D lens activated, view the beads under the photon saturation setting by clicking on **Photon Counts** in the **Image Display** options. Set the initial laser powers to 8.4 mW for the 473 nm laser and to 11.6 mW for the 640 nm laser.

4.5.2 Decrease the focus of the laser to around -300 nm or the focal plane of the calibration beads to produce a clear resolution of the individual beads. Once the z-plane is focused, further adjust the laser power levels to account for variation in each field of view.

4.6 Under the instrument functions, complete 3-D mapping calibration and channel mapping calibration to obtain the errors on the X-, Y-, and Z-axis. Set the max number of FOVs to 20, the target number of points to 4,000, the max distance between channels to 5.0 pixels, and the exclusion radius between channels to 10.0 pixels during channel mapping calibration.

4.7 Ensure that the calibration produces a point coverage of <90% and mapping quality that is good. Save the given calibration data for future image acquisitions.

5 Visualization of EV in three dimensions

5.1 Add 100x oil onto the objective and place the prepared EVs into the microscope. Without the 3-D lens activated, turn on the 640 nm excitation laser and initially raise it to between 1.2 mW and 12.5 mW depending on the intensity of the signal and field of view to excite the red membrane intercalating dye stained EVs.

5.1.1 Under the image display options, switch the viewing method from photon saturation to percentiles to better visualize the EVs. Adjust laser power to minimize noise, while maximizing signal. Maintain all the other parameters.

5.1.2 Adjust the focus of the z-plane by clicking the up or down icon on the Z-axis.

NOTE: The z-plane should be focused between -200 and -350 nm, but will vary depending on the field of view.

5.2 Set the exposure time to 20 ms, the frame capture to 10,000 frames, and the initial laser power to between 1.2 mW and 12.5 mW, or the laser power determined in step 5.1, depending on the intensity of the signal and field of view.

5.2.1 Activate the 3-D lens using the icon and start the acquisition by clicking on the **Acquire** button.

5.3 Throughout image acquisition, raise the laser power by 3 increments of 10 every 1000 frames, or enough to maintain a high signal-to-noise ratio. Do not adjust the z-plane during acquisition.

NOTE: The laser may be raised to a maximum of 90 mW laser power.

6 Post-acquisition modification and EV tracing

6.1 After the image acquisition, toggle over to the **Analyze** viewing window. Perform drift correction on the unfiltered image, and then activate filters. Adjust photon count, localization precision, sigmas, and frame index according to **Table 1**.

6.2 Overlay an XYZ plane view tool along the X-axis of individual EVs from the field of view and export individual .CSV files of photoswitching events.

6.3 Bisect individual EVs on the XY-axis in an X by Y field of view using a line histogram tool, which bins photoswitching events into set distance groups.

6.4 Take images of single EVs and save them as .tiff files.

6.5 Create 3-D videos of individual EVs using a 3-D visualization tool and color according to placement along the Z-axis.

REPRESENTATIVE RESULTS:

The goal of this study was to evaluate the effectiveness of super-resolution microscopy in visualizing individual EVs with nanometer resolution in three dimensions (3-D). To analyze the shape and size of individual EVs, we employed photoswitchable dye and incubated the EVs with a far-red, membrane intercalating dye, and removed excess dye through chromatography²⁹. The

affinity-captured anti-CD81 and red-stained EV were then viewed in the super-resolution microscope under the 640 nm excitation laser. Following the calibration of the microscope that produced an average error of 16 nm on the XY-axis and 38 nm on the Z-axis (**Figure 1A,B**), the purified U2OS EVs were successfully visualized with a resolution of up to 20 nm on the XY-axis and 50 nm along the Z-axis.

Individual EVs visualized through dSTORM in 3-D photoswitched throughout the 10,000 frame exposure as the laser power was increased and were readily apparent in the acquired image (**Figures 2A,B**). Post-acquisition image correction of the Z-plane, photon counts, sigmas, and localization precision of the reconstructed image allowed for the clear resolution of the EV in 3-D (**Figure 2C,D**). The EV in **Figure 2C** photoswitched during only the first 7,000 frames, as seen by the legend in the upper-right corner. This is a result of photobleaching that may have been caused by raising the laser power too quickly. The histogram confirms that the majority of photoswitching events occurred within a 100 nm radius (**Figure 2E**), validating that the visualized EV is an exosome and that the isolation of EVs of a small diameter was successful.

Size distribution analysis was performed on other individually traced EVs using a line histogram tool and XYZ plane view tool to confirm that the majority of photoswitching events occurred within a 100 nm radius of the center (**Figure 3A,C**), further validating dSTORM's ability to visualize EVs of a small diameter. As seen by a 3-D visualization tool, error along the Z-axis is increased, producing an elongated final image of the EV along the axial axis (**Figure 3D, Video 1**). Photoswitching events were not correlated with EV size (**Figure 3E**), demonstrating that dSTORM-based characterization can be used for small EVs such as exosomes and small enveloped viruses less than 100 nm in diameter.

The correct parameters for Z-plane and sigma are integral to the proper resolution of the membrane in 3-D. Additionally, the correct exposure time, number of frames captured, and initial laser level are crucial to producing an image of an individual EV with a resolved membrane. Further investigation should be done on how to optimize the microscope and set both pre and post-acquisitional parameters to capture the highest resolution images of EVs.

FIGURE AND TABLE LEGENDS:

Figure 1: Calibration of the super-resolution microscope in three dimensions using 100 nm microspheres. (A) Field of view in grayscale from calibration of the microscope with microspheres after post-acquisition image corrections. Scale bar in the lower right. (B) Absolute calibration errors on the XY-axis and the Z-axis were obtained through channel mapping calibration and 3-D mapping calibration, respectively. N = 10 biological replicates.

Figure 2: dSTORM of a single EV in three dimensions. (A) Grayscale field of view of CD81+ affinity-purified EVs stained with photoswitchable red membrane intercalating dye and excited with the 640 nm excitation laser. Scale bar in the lower right. (B) Field of view from A labeled according to channel color. (C) Single EV from the zoomed-in view of the white box in A, labeled according to the frame index. The heat map in the upper right indicates the frame in which the

photoswitching events were recorded. Scale bar in the lower right. (D) EV from C labeled according to channel color. (E) Size distribution analysis was created by bisecting the EV on the dashed line shown in D and separating the photoswitching event into 15.4 nm bins using a line histogram tool.

Figure 3: Distribution of photoswitching events during the acquisition of a single EV in three dimensions. (A) Reconstructed image of a CD81+ affinity-purified EV labeled with photoswitchable red membrane intercalating dye and excited with the 640 nm excitation laser. Scale bar in the lower right. (B) Box and whisker plot of average diameters of CD81+ affinity-purified EVs obtained using the microscope's Line Histogram Tool along the XY-axis. (mean = 104 nm, standard deviation = 28 nm). (C) Location of individual photoswitching events along the XY dimension of the EV in A, recorded throughout the 10,000 frame exposure. (D) Location of individual photoswitching events along the XZ-axis of the EV in A, recorded throughout the 10,000 frame exposure. (E) Scatterplot of the number of photoswitching events recorded on individual EVs of varying diameters. R-squared value of 0.1065 demonstrates no correlation between the number of detected photoswitching events and EV diameter.

Video 1: 3-D image of a single CD81+ affinity-purified EV labeled with photoswitchable red membrane intercalating dye and excited with the 640 nm excitation laser. The color scheme is labeled according to depth along the Z-axis. Error along the Z-axis is elongated.

Table 1: Parameters for the super-resolution microscope during 3-D dSTORM acquisition.

DISCUSSION:

EVs have become a popular area of study due to their important role in many intracellular processes and cell-to-cell signaling^{1,30}. However, their visualization proves to be difficult as their small size falls below the diffraction limit of light microscopy. Direct stochastic optical reconstruction microscopy (dSTORM) is a direct method of visualization that bypasses the diffraction limit by capturing photoswitching events of individual fluorophores over time and reconstructing an image based on these blinking events^{21,31}. Super-resolution microscopy has been successfully performed in 3-D on several cellular structures such as actin filaments, microtubules, receptors embedded in the plasma membrane, and viral proteins in infected cells³²⁻³⁶. The purpose of this study was to evaluate the efficacy of super-resolution microscopy, specifically dSTORM, to visualize EVs in 3-D with nanometer resolution. We employed photoswitchable membrane intercalating dye to successfully visualize individual EVs from U2OS cells through dSTORM in up to +/- 20 nm resolution on the XY-axis and +/- 50 nm resolution on the Z-axis. Our previous work has shown that EVs from multiple cell lines and primary fluids have similar size distribution profiles as analyzed by NTA and TEM^{26,37}. The use of a dSTORM-based characterization of EVs can add further confidence to this phenomenon, as well as potentially identify subpopulations in a single field of view. Further refinement of this method is warranted. One notable advantage to dSTORM is that the sample preparation does not require harsh or damaging steps that may alter the structure of the EVs. Our results further demonstrate that the biochemical nature of EVs is maintained during EV purification with anti-CD81 beads and acidic glycine^{26,37}. We fixed the EVs with paraformaldehyde to avoid membrane permeabilizations

caused by other fixatives such as methanol and ethanol. This allowed us to conclude that dSTORM accurately captures the morphology of EVs as they exist in solution. The use of Capto Core 700 is necessary, however, to purify the EVs effectively away from contaminants such as albumin and polyethylene glycol to below regulatory requirements³⁸. One notable limitation of the protocol is that the binding efficiency between the EV and slides is not 100%, so some EVs are lost during sample preparation. Further investigation should be done on the efficacy of adhesive-coated slides to better bind EVs.

While the preparation of EVs for visualization is straightforward, the parameters during acquisition and especially during post-acquisitional modifications vary substantially from sample to sample, depending on the intensity and stability of the EVs and the fluorophore. One area of variability in the experiment is the intensity of the excitation lasers that must be delicately raised throughout exposure to maximize the signal but prevent photobleaching. Photobleaching, or when a fluorophore loses its ability to fluoresce, is a significant limitation throughout super-resolution microscopy^{12,39}. To prevent photobleaching, the concentration of the enzyme in the buffer can be increased to 10 mM to better scavenge oxidizing molecules and prevent photobleaching. Additionally, setting the excitation laser power to a low initial level and slowly raising it throughout exposure to maintain a high signal is critical to prevent photobleaching.

We chose a red photoswitchable dye to stain the EVs due to its excitation wavelength, durability, and ability to withstand fixation²⁹. However, the dye we chose may present issues during super-resolution microscopy when excited too quickly or at too high of an intensity. The fluorophores in the photoswitchable red membrane dye can photobleach after 10,000 frames or after the laser power exceeds 75.6 mW. Additionally, the membrane dye's intensity and ability to fluoresce decreases substantially after a week of storage at 4 °C. Finally, the membrane intercalating dyes have been shown to form micelles in an aqueous solution, so any excess dye still present in the EV sample after purification may be detected and mistaken for an EV if there is no other marker to identify the EV, such as a tetraspanin. Further investigation should be done using other membrane intercalating dyes to optimize for photo-stability^{31,40}. Fluorescent antibodies conjugated to the EV may be a more suitable option as they tend to be more resistant to photobleaching and can amplify the signal⁴¹. However, the drawback of antibodies is that the signal from the fluorophore is slightly offset from the EV due to the distance from the epitope and fluorophore on the antibody.

Existing methods of EV visualization and characterization, such as NTA, flow cytometry, or EM, can require damaging preparation steps or are indirect methods of visualization. dSTORM requires little sample preparation, conserving the natural biochemical nature of EVs, and is a direct method of visualization that can bypass the diffraction limit and visualize EVs of a small diameter^{8–18,21,26}. Other techniques of super-resolution microscopy can be optimized for EV characterization such as stimulated emission depletion (STED), spinning disc confocal microscopy (SDCM), and photo-activated localization microscopy (PALM)^{42,43}. The current study exclusively focuses on dSTORM, but future work on optimizing super-resolution microscopy and comparing/contrasting these techniques is warranted. EVs have recently become a popular area of research as their role in virus progression has become more evident. Many evolutionarily

distinct viruses, such as Epstein Barr Virus, HIV, and Hepatitis A Virus, have evolved to take advantage of the EV-signaling pathways to promote disease progression and evade the body's immune response^{37,44–50}. These viruses have been shown to incorporate viral factors, such as mRNAs or viral proteins, into EVs that can then transfer these components to uninfected cells, while escaping immune detection^{6,51–53}. These exosomal-associated viral factors can be detected and possibly employed as a biomarker for disease progression^{54,55}. Therefore, dSTORM-based visualization of individual EV and their associated proteins can be explored as a platform for disease biomarkers and, perhaps, disease progression of certain viruses^{54,55}. Further research should be done to assess dSTORM's utility in visualizing both contents within an EV and proteins on its membrane.

In conclusion, we have demonstrated that super-resolution microscopy should be considered an effective technique for the visualization of EVs in 3-D with nanometer resolution. Results obtained by dSTORM are consistent with other EV characterizing techniques. A distinct advantage of dSTORM is the ability to directly visualize particles beneath the diffraction limit of light without dehydration or freeze fracture steps that can alter the biochemical nature of EVs.

ACKNOWLEDGMENTS:

We would like to thank Oxford Nanoimaging for their constructive feedback and guidance. This work was funded by the 5UM1CA121947-10 to R.P.M. and the 1R01DA040394 to D.P.D.

DISCLOSURES:

M.C. has no conflicts of interest to declare. R.P.M. and D.P.D. receive material support from Oxford Nanoimaging (ONI) Inc. and Cytiva Inc. (formerly GE Healthcare). R.P.M. and D.P.D. declare competing interests for the possible commercialization of some of the information presented. These are managed by the University of North Carolina. The funding sources were not involved in the interpretations or writing of this manuscript.

REFERENCES:

1. Pegtel, D. M., Gould, S. J. Exosomes. *Annual Review of Biochemistry*. **88**, 487–514 (2019).
2. Raposo, G., Stoorvogel, W. Extracellular vesicles: exosomes, microvesicles, and friends. *The Journal of Cell Biology*. **200** (4), 373–383 (2013).
3. Théry, C., Zitvogel, L., Amigorena, S. Exosomes: composition, biogenesis and function. *Nature Reviews. Immunology*. **2** (8), 569–579 (2002).
4. Coccozza, F., Grisard, E., Martin-Jaular, L., Mathieu, M., Théry, C. SnapShot: Extracellular vesicles. *Cell*. **182** (1), 262–262.e1 (2020).
5. Colombo, M., Raposo, G., Théry, C. Biogenesis, secretion, and intercellular interactions of exosomes and other extracellular vesicles. *Annual Review of Cell and Developmental Biology*. **30**, 255–289 (2014).
6. McNamara, R. P., Dittmer, D. P. Extracellular vesicles in virus infection and pathogenesis. *Current Opinion in Virology*. **44**, 129–138 (2020).
7. Schorey, J. S., Cheng, Y., Singh, P. P., Smith, V. L. Exosomes and other extracellular vesicles in host-pathogen interactions. *EMBO Reports*. **16** (1), 24–43 (2015).
8. Akers, J. C. et al. Comparative analysis of technologies for quantifying Extracellular

441 Vesicles (EVs) in Clinical Cerebrospinal Fluids (CSF). *PLoS One*. **11** (2), e0149866 (2016).

442 9. Maas, S. L. et al. Possibilities and limitations of current technologies for quantification of
443 biological extracellular vesicles and synthetic mimics. *Journal of Controlled Release*. **200**, 87–96
444 (2015).

445 10. Emelyanov, A. et al. Cryo-electron microscopy of extracellular vesicles from cerebrospinal
446 fluid. *PLoS One*. **15** (1), e0227949 (2020).

447 11. Noble, J. M. et al. Direct comparison of optical and electron microscopy methods for
448 structural characterization of extracellular vesicles. *Journal of Structural Biology*. **210** (1), 107474
449 (2020).

450 12. Panagopoulou, M. S., Wark, A. W., Birch, D. J. S., Gregory, C. D. Phenotypic analysis of
451 extracellular vesicles: a review on the applications of fluorescence. *Journal of Extracellular
452 Vesicles*. **9** (1), 1710020 (2020).

453 13. Filipe, V., Hawe, A., Jiskoot, W. Critical evaluation of Nanoparticle Tracking Analysis (NTA)
454 by NanoSight for the measurement of nanoparticles and protein aggregates. *Pharmaceutical
455 Research*. **27** (5), 796–810 (2010).

456 14. Carnell-Morris, P., Tannetta, D., Siupa, A., Hole, P., Dragovic, R. Analysis of extracellular
457 vesicles using fluorescence nanoparticle tracking analysis. *Methods in Molecular Biology*. **1660**,
458 153–173 (2017).

459 15. Dragovic, R. A. et al. Sizing and phenotyping of cellular vesicles using Nanoparticle
460 Tracking Analysis. *Nanomedicine*. **7** (6), 780–788 (2011).

461 16. Bachurski, D. et al. Extracellular vesicle measurements with nanoparticle tracking analysis
462 - An accuracy and repeatability comparison between NanoSight NS300 and ZetaView. *Journal of
463 Extracellular Vesicles*. **8** (1), 1596016 (2019).

464 17. Lacroix, R., Robert, S., Poncelet, P., Dignat-George, F. Overcoming limitations of
465 microparticle measurement by flow cytometry. *Seminars in Thrombosis and Hemostasis*. **36** (8),
466 807–818 (2010).

467 18. Lannigan, J., Erdbruegger, U. Imaging flow cytometry for the characterization of
468 extracellular vesicles. *Methods*. **112**, 55–67 (2017).

469 19. Magenau, A., Gaus, K. 3D super-resolution imaging by localization microscopy. *Methods
470 in Molecular Biology*. **1232**, 123–136 (2015).

471 20. Huang, B., Wang, W., Bates, M., Zhuang, X. Three-dimensional super-resolution imaging
472 by stochastic optical reconstruction microscopy. *Science*. **319** (5864), 810–813 (2008).

473 21. van de Linde, S. et al. Direct stochastic optical reconstruction microscopy with standard
474 fluorescent probes. *Nature Protocols*. **6** (7), 991–1009 (2011).

475 22. Chen, C. et al. Imaging and intracellular tracking of cancer-derived exosomes using single-
476 molecule localization-based super-resolution microscope. *ACS Applied Materials & Interfaces*. **8**
477 (39), 25825–25833 (2016).

478 23. Grant, M. J., Loftus, M. S., Stoja, A. P., Kedes, D. H., Smith, M. M. Superresolution
479 microscopy reveals structural mechanisms driving the nanoarchitecture of a viral chromatin
480 tether. *Proceedings of the National Academy of Sciences of the United States of America*. **115**
481 (19), 4992–4997 (2018).

482 24. Nizamudeen, Z. et al. Rapid and accurate analysis of stem cell-derived extracellular
483 vesicles with super resolution microscopy and live imaging. *Biochimica et Biophysica Acta.
484 Molecular Cell Research*. **1865** (12), 1891–1900 (2018).

- 485 25. Shen, X. et al. 3D dSTORM imaging reveals novel detail of ryanodine receptor localization
486 in rat cardiac myocytes. *The Journal of Physiology*. **597** (2), 399–418 (2019).
- 487 26. McNamara, R. P. et al. Large-scale, cross-flow based isolation of highly pure and
488 endocytosis-competent extracellular vesicles. *Journal of Extracellular Vesicles*. **7** (1), 1541396
489 (2018).
- 490 27. Plotkin, B. J., Sigar, I. M., Swartzendruber, J. A., Kaminski, A. Anaerobic growth and
491 maintenance of mammalian cell lines. *Journal of Visualized Experiments: JoVE*. (137) (2018).
- 492 28. Corso, G. et al. Reproducible and scalable purification of extracellular vesicles using
493 combined bind-elute and size exclusion chromatography. *Science Reports*. **7** (1), 11561 (2017).
- 494 29. Mönkemöller, V. et al. Imaging fenestrations in liver sinusoidal endothelial cells by optical
495 localization microscopy. *Physical Chemistry Chemical Physics*. **16** (24), 12576–12581 (2014).
- 496 30. Mathieu, M., Martin-Jaular, L., Lavieu, G., Théry, C. Specificities of secretion and uptake
497 of exosomes and other extracellular vesicles for cell-to-cell communication. *Nature Cell Biology*.
498 **21** (1), 9–17 (2019).
- 499 31. Wang, L., Frei, M. S., Salim, A., Johnsson, K. Small-molecule fluorescent probes for live-
500 cell super-resolution microscopy. *Journal of the American Chemical Society*. **141** (7), 2770–2781
501 (2019).
- 502 32. Hu, Y. S., Cang, H., Lillemeier, B. F. Superresolution imaging reveals nanometer- and
503 micrometer-scale spatial distributions of T-cell receptors in lymph nodes. *Proceedings of the*
504 *National Academy of Sciences of the United States of America*. **113** (26), 7201–7206 (2016).
- 505 33. Jayasinghe, I. et al. True molecular scale visualization of variable clustering properties of
506 ryanodine receptors. *Cell Reports*. **22** (2), 557–567 (2018).
- 507 34. Eggert, D., Rösch, K., Reimer, R., Herker, E. Visualization and analysis of hepatitis C virus
508 structural proteins at lipid droplets by super-resolution microscopy. *PLoS One*. **9** (7), e102511
509 (2014).
- 510 35. Mazloom-Farsibaf, H. et al. Comparing lifeact and phalloidin for super-resolution imaging
511 of actin in fixed cells. *PLoS One*. **16** (1), e0246138 (2021).
- 512 36. Huang, B., Jones, S. A., Brandenburg, B., Zhuang, X. Whole-cell 3D STORM reveals
513 interactions between cellular structures with nanometer-scale resolution. *Nature Methods*. **5**
514 (12), 1047–1052 (2008).
- 515 37. McNamara, R. P. et al. Nef secretion into extracellular vesicles or exosomes is conserved
516 across human and simian immunodeficiency viruses. *mBio* **9** (1), e02344 (2018).
- 517 38. Blom, H. et al. Efficient chromatographic reduction of ovalbumin for egg-based influenza
518 virus purification. *Vaccine*. **32** (30), 3721–3724 (2014).
- 519 39. Kalies, S., Kuetemeyer, K., Heisterkamp, A. Mechanisms of high-order photobleaching and
520 its relationship to intracellular ablation. *Biomedical Optics Express*. **2** (4), 805–816 (2011).
- 521 40. Mönkemöller, V., Øie, C., Hübner, W., Huser, T., McCourt, P. Multimodal super-resolution
522 optical microscopy visualizes the close connection between membrane and the cytoskeleton in
523 liver sinusoidal endothelial cell fenestrations. *Scientific Reports*. **5**, 16279 (2015).
- 524 41. Xu, J., Ma, H., Liu, Y. Stochastic Optical Reconstruction Microscopy (STORM). *Current*
525 *Protocols in Cytometry*. **81**, 12.46.1–12.46.27 (2017).
- 526 42. Godin, A. G., Lounis, B., Cognet, L. Super-resolution microscopy approaches for live cell
527 imaging. *Biophysical Journal*. **107** (8), 1777–1784 (2014).
- 528 43. Azuma, T., Kei, T. Super-resolution spinning-disk confocal microscopy using optical

529 photon reassignment. *Optics Express*. **23** (11), 15003–15011 (2015).

530 44. Hurwitz, S. N. et al. CD63 regulates Epstein-Barr Virus LMP1 exosomal packaging,
531 enhancement of vesicle production, and noncanonical NF- κ B signaling. *Journal of Virology*. **91** (5),
532 e02251–16 (2017).

533 45. Hurwitz, S. N., Cheerathodi, M. R., Nkosi, D., York, S. B., Meckes, D. G. Tetraspanin CD63
534 bridges autophagic and endosomal processes to regulate exosomal secretion and intracellular
535 signaling of Epstein-Barr Virus LMP1. *Journal of Virology*. **92** (5), e01969–17 (2018).

536 46. Bukong, T. N., Momen-Heravi, F., Kodys, K., Bala, S., Szabo, G. Exosomes from hepatitis C
537 infected patients transmit HCV infection and contain replication competent viral RNA in complex
538 with Ago2-miR122-HSP90. *PLoS Pathogens*. **10** (10), e1004424 (2014).

539 47. Khan, M. B. et al. Nef exosomes isolated from the plasma of individuals with HIV-
540 associated dementia (HAD) can induce A β (1-42) secretion in SH-SY5Y neural cells. *J*
541 *Neurovirology*. **22** (2), 179–190 (2016).

542 48. Lee, J. H. et al. HIV-Nef and ADAM17-containing plasma extracellular vesicles induce and
543 correlate with immune pathogenesis in chronic HIV infection. *EBioMedicine* **6**, 103–113 (2016).

544 49. Meckes, D. G. et al. Modulation of B-cell exosome proteins by gamma herpesvirus
545 infection. *Proceedings of the National Academy of Sciences of the United States of America*. **110**
546 (31), E2925–33 (2013).

547 50. Raymond, A. D. et al. Microglia-derived HIV Nef+ exosome impairment of the blood-brain
548 barrier is treatable by nanomedicine-based delivery of Nef peptides. *Journal of Neurovirology*. **22**
549 (2), 129–139 (2016).

550 51. Raab-Traub, N., Dittmer, D. P. Viral effects on the content and function of extracellular
551 vesicles. *Nature Reviews Microbiology*. **15** (9), 559–572 (2017).

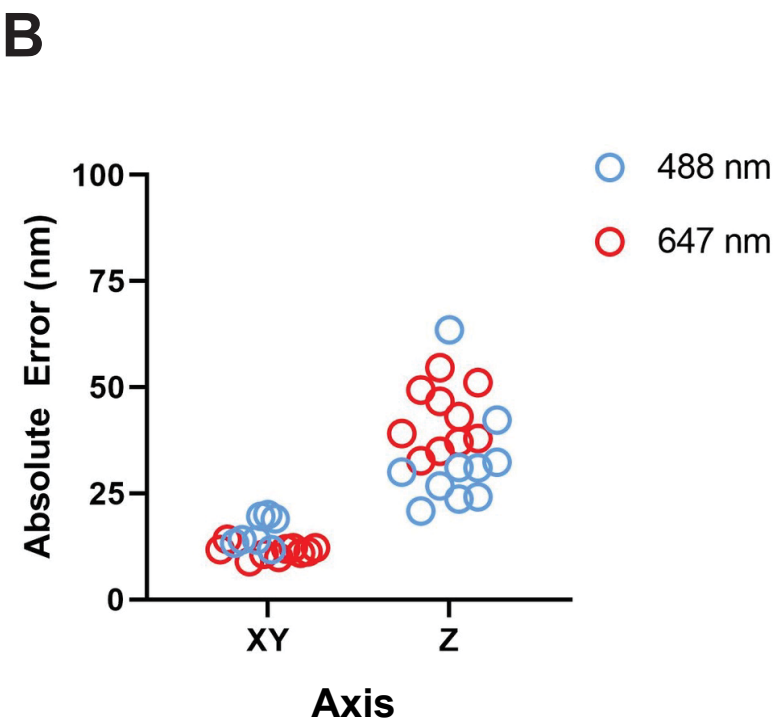
552 52. Feng, Z. et al. A pathogenic picornavirus acquires an envelope by hijacking cellular
553 membranes. *Nature*. **496** (7445), 367–371 (2013).

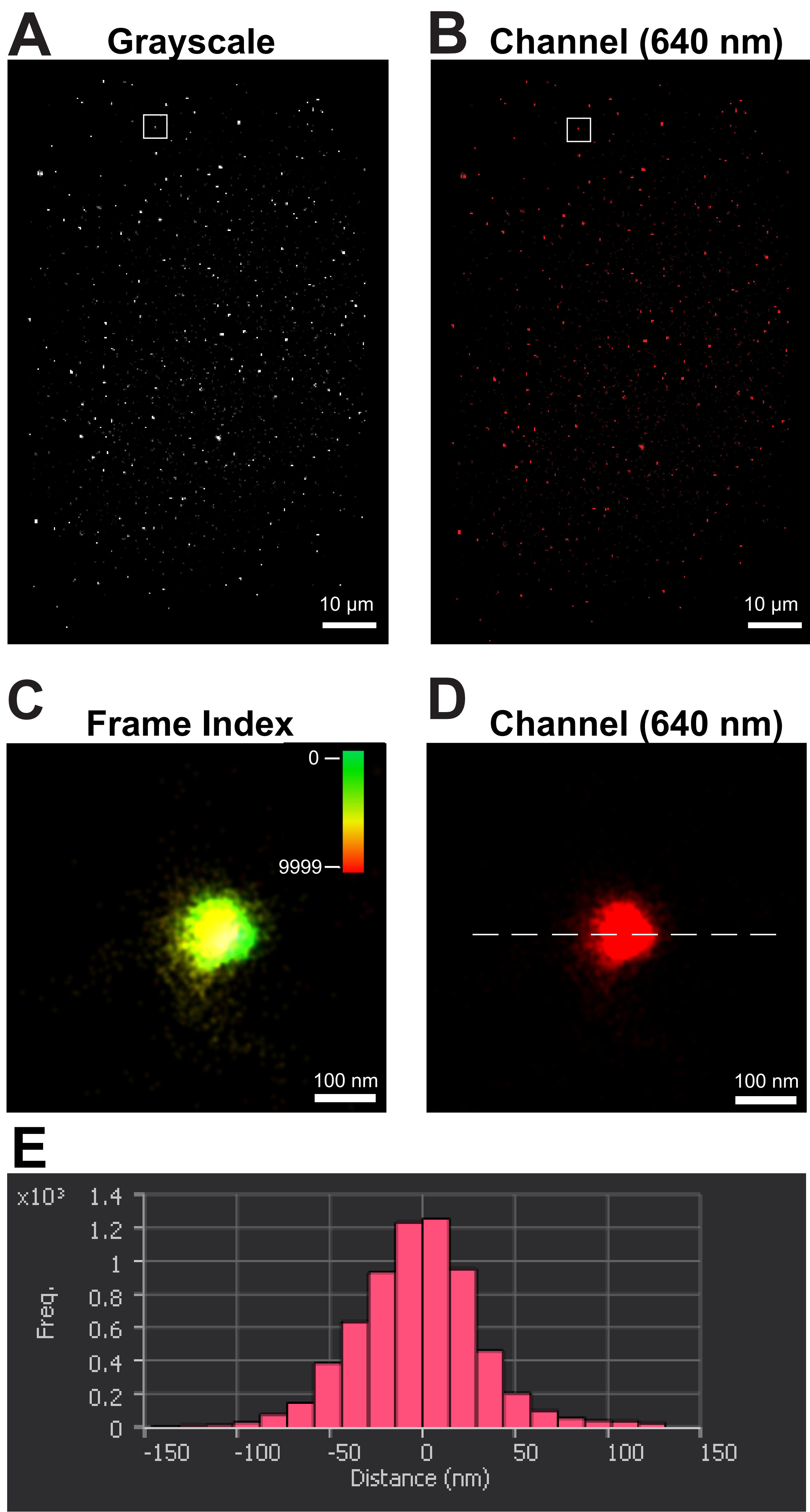
554 53. Bandopadhyay, M., Bharadwaj, M. Exosomal miRNAs in hepatitis B virus related liver
555 disease: a new hope for biomarker. *Gut Pathogens*. **12**, 23 (2020).

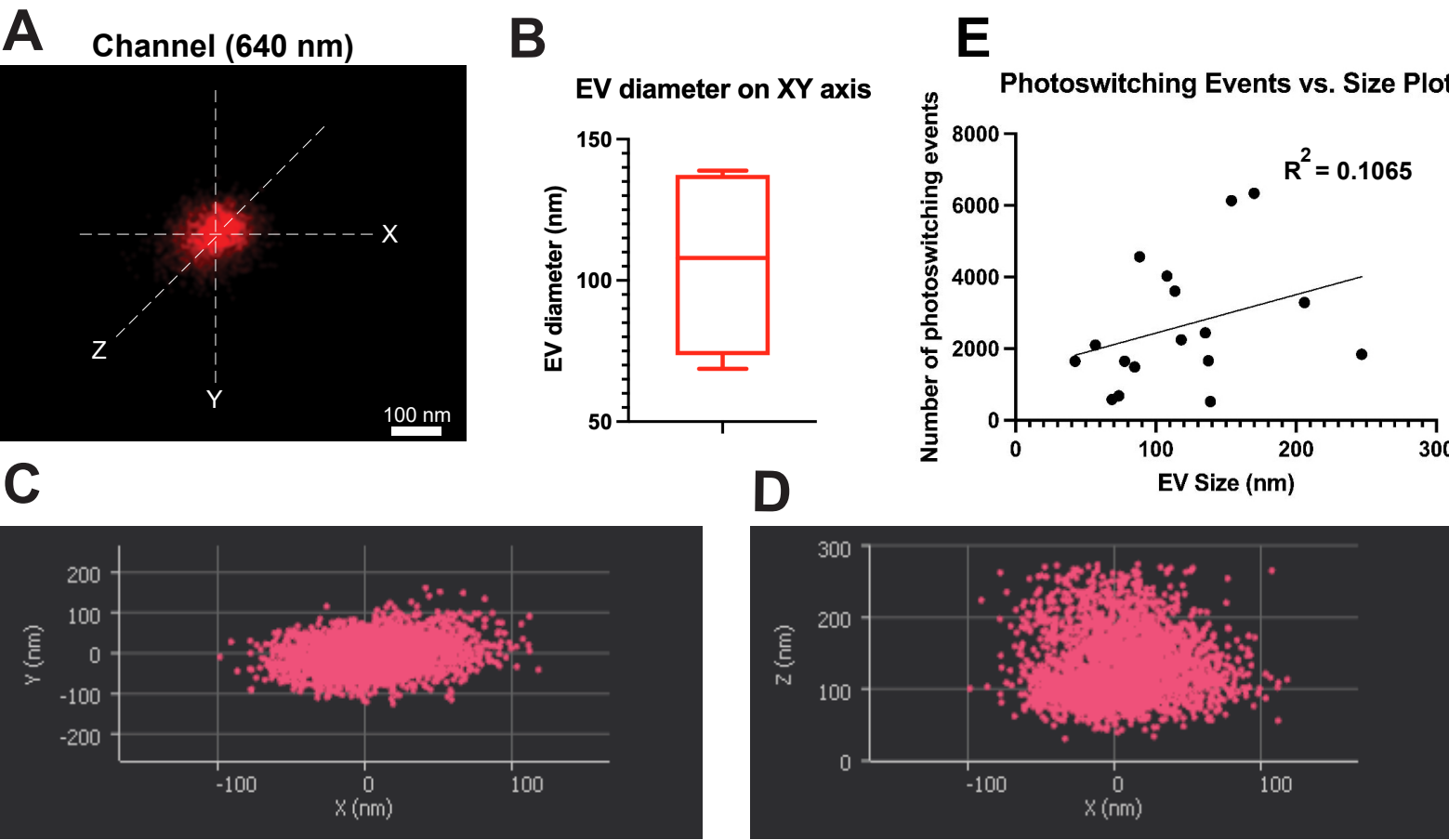
556 54. Hurwitz, S. N. et al. Proteomic profiling of NCI-60 extracellular vesicles uncovers common
557 protein cargo and cancer type-specific biomarkers. *Oncotarget*. **7** (52), 86999–87015 (2016).

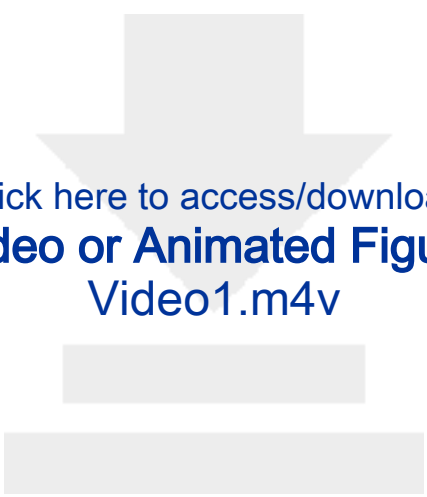
558 55. Rodrigues, M., Fan, J., Lyon, C., Wan, M., Hu, Y. Role of extracellular vesicles in viral and
559 bacterial infections: Pathogenesis, diagnostics, and therapeutics. *Theranostics*. **8** (10), 2709–2721
560 (2018).

561









Click here to access/download
Video or Animated Figure
Video1.m4v



Click here to access/download

Table of Materials

JoVE_Materials_RPM.xls



Dear Dr. Dittmer,

Your manuscript, JoVE62845 "Direct Stochastic Optical Reconstruction Microscopy of Extracellular Vesicles in Three Dimensions," has been editorially and peer reviewed, and the following comments need to be addressed. Note that editorial comments address both requirements for video production and formatting of the article for publication. Please track the changes within the manuscript to identify all of the edits.

After revising and uploading your submission, please also upload a separate rebuttal document that addresses each of the editorial and peer review comments individually.

Your revision is due by **Jun 08, 2021**.

To submit a revision, go to the [JoVE submission site](#) and log in as an author. You will find your submission under the heading "Submission Needing Revision". Please note that the corresponding author in Editorial Manager refers to the point of contact during the review and production of the video article.

Best,

Vineeta Bajaj, Ph.D.
Review Editor
JoVE
vineeta.bajaj@jove.com
617.674.1888
Follow us: Facebook | Twitter | LinkedIn
About JoVE

Editorial comments:

Changes to be made by the Author(s):

1. Please take this opportunity to thoroughly proofread the manuscript to ensure that there are no spelling or grammar issues.

We have corrected all spelling and grammar issues throughout the manuscript.

2. Please provide an email address for each author.

Email addresses for each author have now been included on lines 8-9.

3. Please ensure that the long Abstract is within 150-300-word limit and clearly states the goal of the protocol.

The long abstract is 115 words and we are content with it as it stands.

4. JoVE cannot publish manuscripts containing commercial language. This includes trademark symbols (™), registered symbols (®), and company names before an instrument or reagent. Please remove all commercial language from your manuscript and use generic terms instead. All commercial products should be sufficiently referenced in the Table of Materials and Reagents.

For example: CellMask Red, AKTA Flux X, AKTA Start, Frac 30, HiTrap Capto Core 700, Dynabeads, ONI Nanoimager, etc.

All trademark symbols, registered symbols, and company names before an instrument or reagent have been removed. The Table of Materials and Reagents has also been updated to address this.

5. Please revise the following lines to avoid overlap with previously published work: 142-153,

Lines 153-166, or the caution statement for paraformaldehyde, has been removed to avoid overlap with previously published work.

6. Please ensure that all text in the protocol section is written in the imperative tense as if telling someone how to do the technique (e.g., “Do this,” “Ensure that,” etc.). The actions should be described in the imperative tense in complete sentences wherever possible. Avoid usage of phrases such as “could be,” “should be,” and “would be” throughout the Protocol. Any text that cannot be written in the imperative tense may be added as a “Note.”

The protocol was rewritten in the imperative tense and in complete sentences. Steps that couldn't be written in the imperative were included as “Notes” in steps 1.1, 3.4.1, 4.4, 5.1.2, and 5.3.

7. Please ensure that individual steps of the protocol should only contain 2-3 action sentences per step.

Steps of the protocol were adjusted to only include 2-3 action sentences per step. Extra steps were added to accommodate the changes made to the existing steps. Specifically, steps 2.2.2, 3.4.1, 4.1.1, 4.3, 4.4, and 4.5.1-4.6 were inserted, and steps 5.1-5.2.1 were adjusted to accommodate these changes. Finally, step 2.2 was removed due to redundancy in step 2.3.

8. Please note that your protocol will be used to generate the script for the video and must contain everything that you would like shown in the video. Please add more details to your protocol steps. Please ensure you answer the “how” question, i.e., how is the step performed? Alternatively, add references to published material specifying how to perform the protocol action. Please add more specific details (e.g., button clicks for software actions, numerical values for settings, etc) to your protocol steps. There should be enough detail in each step to supplement the actions seen in the video so that viewers can easily replicate the protocol.

Additional detail specifying how the protocol is performed was inserted in steps 3.4, 4.3, 4.5-4.6, and 5.1-5.3. Moreover, references were inserted in steps 1.1, 1.2, 2.2.1, 2.6, and 3.2 to specify how steps of the protocol were performed. We believe there is now enough detail in each step to effectively supplement actions that will be seen in the video.

9. There is a 10-page limit for the Protocol, but there is a 3-page limit for filmable content. Please highlight 3 pages or less of the Protocol (including headings and spacing) that identifies the essential steps of the protocol for the video, i.e., the steps that should be visualized to tell the most cohesive story of the Protocol.

The highlighted protocol was moved to lines 145 to 163 and 182 to 229 in order to better identify the most essential steps of the protocol and to demonstrate how the microscope should be used. To allow for the three-page limit, we did not highlight sections 4.1 – 4.3.

10. Please ensure the results are described in the context of the presented technique. e.g., how do these results show the technique, suggestions about how to analyze the outcome, etc. The paragraph text should refer to all of the figures. Data from both successful and sub-optimal experiments can be included.

A short explanation of Figure 1 was inserted in lines 256-257 to explicitly mention the average calibration errors found for 3-D dSTORM. Additionally, a description of sub-optimal results seen in Figure 2C was inserted in lines 264-267. Moreover, an explanation interpreting the distributions seen in Figures 2 and 3 are included throughout the results. Finally, a plot demonstrating detection sensitivity related to the size of the EV was created and inserted in Figure 3, so a short description of Figure 3E was also inserted into the results on lines 276-279.

11. Please obtain explicit copyright permission to reuse any figures from a previous publication. Explicit permission can be expressed in the form of a letter from the editor or a link to the editorial policy that allows re-prints. Please upload this information as a

.doc or .docx file to your Editorial Manager account. The Figure must be cited appropriately in the Figure Legend, i.e. "This figure has been modified from [citation]."

The figures presented are not reused from a previous publication and therefore do not require explicit copyright permission.

12. As we are a methods journal, please ensure that the Discussion explicitly cover the following in detail in 3-6 paragraphs with citations:

- a) Critical steps within the protocol
- b) Any modifications and troubleshooting of the technique
- c) Any limitations of the technique
- d) The significance with respect to existing methods
- e) Any future applications of the technique

We have reviewed and edited the discussion section to ensure that all of these criteria are met. To review, we addressed the most critical step of the protocol and highlighted its importance in lines 364-367 and 370-372. Additionally, modifications to the staining method to produce better images are discussed in lines 376-389, including discussions on the pros and cons of alternative labeling methods (lines 384-388). The significance of dSTORM with respect to existing methods was mentioned in the introduction, as well as in lines 390-394 of the discussion. Additionally, a comparison of dSTORM and other super-resolution techniques has been inserted in lines 394-399. Future applications of dSTORM are also discussed in lines 399-411.

Reviewers' comments:

Reviewer #1:

Manuscript Summary:

The current manuscript titled "Direct Stochastic Optical Reconstruction Microscopy of Extracellular Vesicles in Three Dimensions" describes use of super-resolution microscopy such as direct stochastic optical reconstruction microscopy (dSTORM) which utilizes photo-switchable of specific fluorophores to reconstruct nanometer images. The overall goal was to evaluate the effectiveness of super-resolution microscopy in visualizing individual EVs with nanometer resolution in three dimensions (3-D). Here they have employed photo-switchable membrane dye by incubating the EVs with CellMask Red and removing excess dye through chromatography. The affinity-captured anti-CD81 and CellMask Red stained EV were then viewed in the Nanoimager under the 640 nm excitation laser. Overall, this is an interesting and novel method of EV detection which is highly sensitive and much needed in the EV field.

We thank this reviewer for their positive assessment of our manuscript and have addressed their major and minor concerns below.

Major Concerns:

There are, however, few concerns that include:

1. It would be important to document the state of U2OAs cells prior to EV isolation. Are the cells at early/mid log phase of growth or stationary phase? An MTT assay would be critical to show this.

We continuously passage the cells to maintain them in mid-log phase and prevent them from entering the stationary phase. A description of this process was inserted in step 1.2 to highlight the state of cells prior to EV isolation.

2. The authors should try multiple cell types including primary cells for rigor and reproducibility of their results.

Others and our previous work have demonstrated that the overall size and structure of EVs are consistent across cell types, as well as in primary fluids (PMID: 29437924). Therefore, we are confident that the dSTORM platform will reflect this as well, but the reviewer is correct that this could be a caveat. We have added a short explanation addressing this concern was inserted in lines 344-348 in the discussion.

Minor Concerns:

None

Reviewer #2:

Manuscript Summary:

This is a well written protocol that describes the use of dSTORM super resolution microscopy for visualization and characterization of EVs.

We thank the reviewer for their positive feedback on this manuscript. We have addressed their minor concerns below.

Major Concerns:

None

Minor Concerns: A few minor suggestions include:

1) What is the efficiency of dissociation of EVs from the anti-CD81 magnetic beads? Will this process affect the biochemical nature of EVs as it may cause dissociation of surface anchored cargo?

The exact efficiency of dissociation of EVs from anti-CD81 beads is unknown. However, it has been shown that the dissociation of EVs from anti-CD81 beads using acidic

glycine does not affect the biochemical nature of EVs and that the functionality of EVs is maintained after this process. We inserted an explanation of this with relevant references in lines 350-352.

2) What is the MW of the PEG used? How efficiently is the PEG removed?

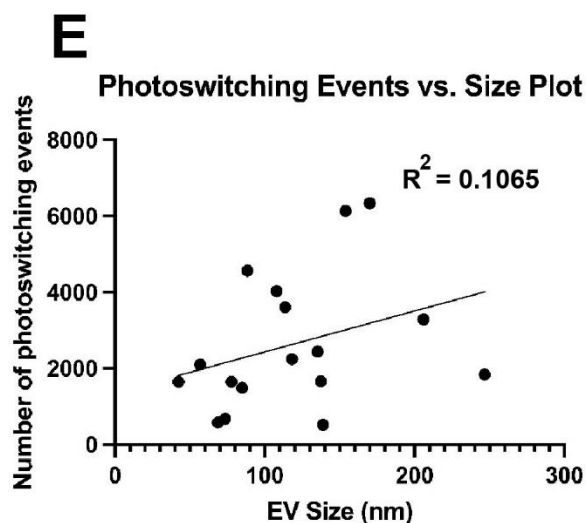
The molecular weight of the PEG used is 8000 Da. The protocol has been updated to reflect this. The Capto Core 700 column used in this protocol was developed specifically to remove contaminants such as PEG and albumin, and was based on developmental protocols using Capto Core 700 (PMID: 24801053), we conclude that removal is greater than 95%, and the final EV solution. A statement reflecting this was inserted in lines 355-357 of the discussion.

3) Why calibration was done with 100 nm microspheres and not with smaller microspheres as well?

The microscope was calibrated according to the manufacturer's protocol with the beads provided, which were 100 nm microspheres. Additionally, the average size of an exosome is around 100 nm, so 100 nm microspheres are sufficient to calibrate the microscope when viewing EVs.

4) As the size of EVs drops below 100 nm how the detection sensitivity changes?

This is an excellent question by the reviewer. We have found that detection sensitivity is not correlated with the size of the EV. We acknowledge this is a significant question, and therefore inserted the scatterplot below of photoswitching events versus size of the EV as a newly incorporated Figure 3E. As seen by the R^2 value of 0.1065, size and detection sensitivity do not correlate. Therefore, as the size of the EV drops below 100 nm detection sensitivity does not significantly drop. We inserted an explanation of this in lines 276-279 in the results section.



5) Is there any particular advantage of dSTORM over STED or spinning disk super resolution confocal microscopy? How do they compare?

This is an excellent point by the reviewer. dSTORM is only one flavor of super-resolution microscopy. Other approaches include stimulated emission depleted (STED) microscopy, spinning disk confocal super-resolution microscopy, structured illuminated microscopy (SIM), and photo-activated localization microscopy (PALM). While we agree a side-by-side comparison with these other techniques for EV imaging is necessary, we believe it is beyond the scope of our current manuscript as our goal was to establish a protocol only applicable for dSTORM. We have included a brief introduction to these other techniques in our discussion and look forward to future studies using these other super-resolution characterization methods (lines 394-399).

Reviewer #3:

Manuscript summary:

There are currently limited means of analyzing extracellular vesicles (EVs) at single vesicle resolution. The manuscript by Chambers and colleagues provides a novel and detailed method of using super-resolution microscopy (dStorm) to visualize EVs in 3D. This method and video will be of broad benefit to those studying EVs and even viruses. It could easily be expanded to monitor distinct molecular markers for analyzing EV subtypes a major challenge in the field. I have a few comments and suggestions that may help improve the manuscript:

We thank the reviewer for their positive assessment of our article and agree that there are limited means of directly studying/analyzing EVs. We have addressed the reviewer's concerns below.

1. Section 1.1, could the authors explain how they generated the EV-free FBS? Or was it purchased that way from a commercial source?

The exosome-free FBS was generated using PEG precipitation to remove the EVs. A reference has been inserted in step 1.1 to demonstrate how the FBS was prepared.

2. Section 2.2, why was a 750kDa cut-off filter chosen? Would small EVs be lost with this size cut-off? I thought 100kDa filters are used to retain small EVs (i.e., exosomes).

The 750 kDa cut-off filter was chosen during EV isolation because this size filter has been shown to retain small EVs at nearly the same rate as smaller cut-off filters while removing proteins, metabolites, and other cellular debris more efficiently than the smaller cut-off filters (PMID: 30533204). Therefore, while we acknowledge the

reviewer's concern that some EV loss can occur during the process, we feel it is necessary to remove items less than 750 kDa during purification for the highly sensitive dSTORM-based analysis. A reference was inserted in step 2.2 to demonstrate the effectiveness of this size filter in EV purification.

3. Section 2.5, what molecular weight is the PEG and is the concentration listed the final concentration in the media for precipitation?

The molecular weight of the PEG is 8000 Da, and the concentration listed in the protocol is the final concentration of PEG in the media for precipitation. Step 2.4 has been updated to include the molecular weight of the PEG used and to articulate that 40 mg/mL is the final concentration of PEG.

4. Section 3.3, are the slides coated with anything? How do the authors think the EVs attach? Do you have any idea of the binding efficiency?

The slides used here are not coated with anything. We conclude that there is some natural affinity of EV surface proteins to the glass slides, but the exact binding efficiency is unknown because it is a heterogeneous population of EVs. We have inserted a brief mention of the efficacy of adhesive slides in lines 357-360 of the discussion.

5. The authors describe paraformaldehyde fixation. Do other means of fixation work in with this protocol?

We chose paraformaldehyde as the fixative for this protocol because we didn't want to permeabilize the EVs which would disrupt their structure. Therefore, other fixatives that permeabilize the EV membrane such as methanol and ethanol would not be ideally suited for this protocol. A brief explanation for the rationale behind using paraformaldehyde as the fixative was inserted in lines 352-354.



**LINEBERGER COMPREHENSIVE
CANCER CENTER**

Campus Box 7295
Chapel Hill, NC 27599-7295
unclineberger.org

Designated a comprehensive cancer center by the National Cancer Institute

☎ 919-966-3036 · 📠 919-962-8472

Dirk P. Dittmer, Ph.D.

Professor, Dept. of Microbiology and Immunology
Team Lead for Programs in Virology and Global Oncology
Director UNC Vironomics Core DDITTMER@MED.UNC.EDU

Dear Benjamin Werth,

Enclosed, please find our invited submission titled “*Direct Stochastic Optical Reconstruction Microscopy of Extracellular Vesicles in Three Dimensions*” for consideration in *the Journal of Visualized Experiments*.

Extracellular vesicles (EVs) or exosomes are intimately involved in gene regulation and cell signaling and thus play an integral role in organismal homeostasis. The visualization and biophysical characterizations of EVs have become a popular area of research; however, due to their small size falling below the diffraction limit, visualization of EVs has proven difficult.

Here, we present our workflow on the resolving of individual EVs through super-resolution imaging, namely direct stochastic optical reconstruction microscopy (dSTORM). This approach can be used to visualize single EV morphology in all three dimensions. It yields the most physiologically relevant visualizations yet, by avoiding dehydration and freeze-fracture steps, high-speed centrifugation, and stringent fixation.

In conclusion, we propose that dSTORM be considered a reproducible and scalable method for the characterization of EVs.

We thank you very much for your time and consideration.

Sincerely,



Dirk Dittmer, Ph.D.